



This is a repository copy of *A review of Pochhammer-Chree dispersion in the Hopkinson bar*.

White Rose Research Online URL for this paper:
<http://eprints.whiterose.ac.uk/129444/>

Version: Accepted Version

Article:

Rigby, S., Barr, A.D. orcid.org/0000-0002-8240-6412 and Clayton, M. (2018) A review of Pochhammer-Chree dispersion in the Hopkinson bar. *Proceedings of the Institution of Civil Engineers-Engineering and Computational Mechanics*, 171 (1). pp. 3-13. ISSN 1755-0777

<https://doi.org/10.1680/jencm.16.00027>

Reuse

Items deposited in White Rose Research Online are protected by copyright, with all rights reserved unless indicated otherwise. They may be downloaded and/or printed for private study, or other acts as permitted by national copyright laws. The publisher or other rights holders may allow further reproduction and re-use of the full text version. This is indicated by the licence information on the White Rose Research Online record for the item.

Takedown

If you consider content in White Rose Research Online to be in breach of UK law, please notify us by emailing eprints@whiterose.ac.uk including the URL of the record and the reason for the withdrawal request.



eprints@whiterose.ac.uk
<https://eprints.whiterose.ac.uk/>

Date

October 23, 2017

Title

A review of Pochhammer-Chree dispersion in the Hopkinson bar

Authors

Sam E. Rigby, MEng, PhD

Lecturer in Blast & Impact Engineering, University of Sheffield, Sheffield, UK

Andrew D. Barr, MEng, PhD

Research Associate, University of Sheffield, Sheffield, UK

Max Clayton, MEng

Postgraduate Research Assistant, University of Sheffield, Sheffield, UK

Corresponding Author

Sam E. Rigby

University of Sheffield

Department of Civil & Structural Engineering

Sir Frederick Mappin Building

Mappin Street

Sheffield

S1 3JD

E: sam.rigby@sheffield.ac.uk

T: +44 (0)114 222 5724

Number of Words

approx. 4200

Number of Tables

1

Number of Illustrations

8

Abstract

This paper presents a detailed review of the current state-of-the-art in Hopkinson pressure bar (HPB) data analysis. In particular, the underlying theory of the HPB is discussed, and methods of correcting signals for Pochhammer-Chree dispersion and other associated effects are described. The theory of multiple mode propagation is presented, followed by a review of current methods for correcting multiple mode dispersion, which are especially pertinent when using the HPB as a dynamic force transducer to measure rapidly changing loading events such as explosive blast loads.

Keywords

Computational Mechanics; Mathematical Modelling; Solid Mechanics

A review of Pochhammer-Chree dispersion in the Hopkinson bar

Review paper

Sam E. Rigby, Andrew D. Barr & Max Clayton
Dept. Civil & Structural Engineering, University of Sheffield, UK.

October 23, 2017

Abstract

This paper presents a detailed review of the current state-of-the-art in Hopkinson pressure bar (HPB) data analysis. In particular, the underlying theory of the HPB is discussed, and methods of correcting signals for Pochhammer-Chree dispersion and other associated effects are described. The theory of multiple mode propagation is presented, followed by a review of current methods for correcting multiple mode dispersion, which are especially pertinent when using the HPB as a dynamic force transducer to measure rapidly changing loading events such as explosive blast loads.

Notation

a	-	bar radius
A	-	cross-sectional area
C_0	-	longitudinal wave velocity
C_g	-	group velocity
C_p	-	phase velocity
E	-	(static) Young's modulus of elasticity
f	-	frequency of oscillation
F	-	force
$J_n(y)$	-	Bessel function of the first kind, order n
L	-	wavelength of oscillation
m	-	mass
M_1	-	correction factor to convert surface axial strain to average axial strain over the cross-section
M_2	-	correction factor to convert average axial strain to average axial stress
u	-	axial displacement
\ddot{u}	-	axial acceleration
z	-	axial ordinate of location on bar
γ	-	wave number, $\gamma = 2\pi/L$
ν	-	Poisson's ratio
ρ	-	density
σ_z	-	axial stress
ϕ	-	phase angle
ϕ'	-	phase shift
ϕ_{corr}	-	phase angle correction

1 Introduction

Detonation of a high explosive results in a near-instantaneous release of energy. As the extremely high-energy and high-pressure detonation products violently expand, they displace the surrounding air and cause a shock

wave to form, which propagates away from the source at velocities several times greater than the speed of sound. This blast wave has the potential to cause catastrophic damage to any obstacles that it encounters.

Over recent years, blast resilient design has moved increasingly into the civilian domain. Where blast resilience was previously only considered for high-value buildings such as embassies, forward operating bases, and political and military headquarters, counter-terrorist measures are an increasingly common consideration in infrastructure projects (Cormie et al. 2009). A primary challenge that faces the blast protection community is accurate quantification of the loading that a building component will be subjected to. Whilst the loading can be determined for the most simple geometrical situations using well-established semi-empirical predictive methods (Hyde 1991, US Department of Defence 2008) or finite element/computational fluid dynamics solvers, there are questions over the applicability of such methods for complex scenarios such as extremely close-in blast events (Shin et al. 2014, 2015).

Existing instruments and sensors are either too fragile or lack the sensitivity to properly measure the loading at such a short distances from a high explosive detonation. Owing to this, there is a lack of well-controlled, detailed measurement of blast parameters in the domain close to a charge. Bertram Hopkinson (1914) developed an experimental method for accurate measurement of high-energy, transient loads. This apparatus, based on the theory of elastic stress wave propagation, has since been termed the Hopkinson pressure bar (HPB) and will be detailed in later sections. An adaptation of this technique (Clarke et al. 2015) has recently been used by researchers at the University of Sheffield to measure the loading from both near-field (Rigby et al. 2015) and buried explosive events (Rigby et al. 2016), as well as the dynamic deformation of explosively loaded plates Fay et al. (2015).

Whilst the HPB technique has many advantages, it also has a number of limitations. This article reviews the state-of-the-art of the HPB, with a specific focus on its use as a dynamic force transducer, and draws on both historical and current efforts to improve our theoretical treatment of the HPB. The applications and limitations of the HPB are discussed in a civil engineering context.

2 One-dimensional elastic wave propagation

This section presents an abridged version of the derivation presented in Kolsky (1963), where the reader is directed to for a more detailed theoretical treatment of stress wave propagation in bounded elastic media.

In classical mechanics it is assumed that after application of a force F , an object of mass m is accelerated immediately with uniform magnitude acceleration \ddot{u} throughout its body (i.e. the expression $F = m\ddot{u}$ holds true for the entire body). This is a reasonable assumption if the loading is applied gradually, however with rapid transient events there must be a delay between the load being applied and the information of the loading reaching a point located some distance from the area where the load is applied. We must therefore consider the propagation of stress *through* an object.

Consider a one-dimensional element within an elastic bar, of length ∂z , located at a distance z from the loaded face of the bar (Figure 1). As a stress wave propagates over the element, the element becomes strained and changes in length. If the axial displacement at the proximal face of the element (the face nearest the loaded end of the bar) is given as u , then the displacement at distal face (the face furthest from the loaded end of the bar) is given as

$$u + \frac{\partial u}{\partial z} \partial z \quad (1)$$

when taking tensile strain, $\partial u/\partial z$, as positive. The length of the stressed element is now given as

$$\partial z + \left(u + \frac{\partial u}{\partial z} \partial z \right) - u = \partial z + \frac{\partial u}{\partial z} \partial z. \quad (2)$$

Assuming that the element remains elastic, the axial stress in the element is

$$\sigma_z = E \frac{\partial u}{\partial z} \quad (3)$$

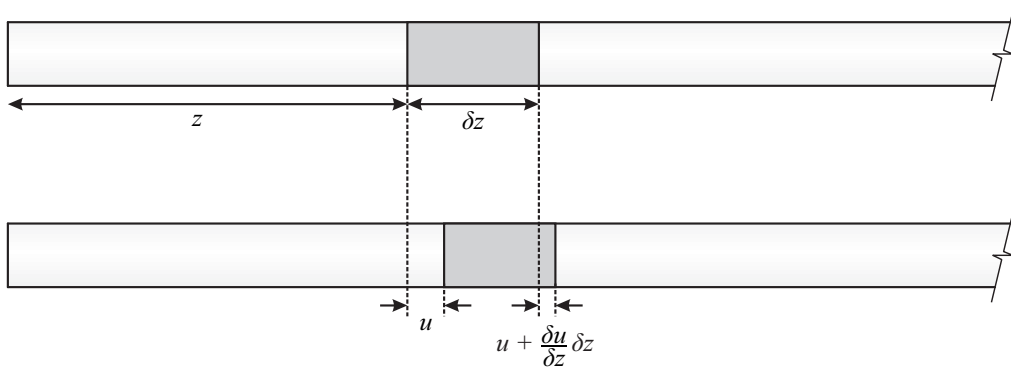


Figure 1: Displacement of an element within a one-dimensional bar after being subjected to a propagating elastic stress wave

where E is the Young's modulus of the bar. The net axial force is given as the force acting on the distal end minus the force acting on the proximal end of the element,

$$A \left(\sigma_z + \frac{\partial \sigma_z}{\partial z} \partial z \right) - A \sigma_z = A \frac{\partial \sigma_z}{\partial z} \partial z \quad (4)$$

where σ_z is axial stress and A is cross-sectional area. The mass of the element is $\rho A \partial z$, where ρ is density, and the axial acceleration is $\partial^2 u / \partial t^2$, where t is time. By Newton's Second Law, the product of these two must equal the net force in the element, i.e.

$$\rho A \partial z \frac{\partial^2 u}{\partial t^2} = A \frac{\partial \sigma_z}{\partial z} \partial z. \quad (5)$$

Substituting from equation 3 into equation 5 gives

$$\frac{\partial^2 u}{\partial t^2} = \frac{E}{\rho} \frac{\partial^2 u}{\partial z^2}. \quad (6)$$

This is the well-known one-dimensional wave equation describing the propagation of a stress pulse through a bar. According to the equation above, a stress disturbance will travel through the bar at a velocity of $C_0 = \sqrt{E/\rho}$, where C_0 is known as the longitudinal wave velocity, or the bar velocity.

3 Applications of the Hopkinson pressure bar

3.1 Hopkinson pressure bars

The HPB technique, originally devised by Hopkinson (1914) and later developed by Robertson (1921) and Landon & Quinney (1923), is based on elastic stress wave theory as described above. After a bullet, or shock wave emanating from a detonated explosive, impacts the end of a cylindrical bar, a compressive wave travels through the material. When used in this manner, the HPB acts as a robust, dynamic force transducer. In its original form, a short length of the distal end of the HPB (known as the time-piece) was machined off and re-attached using a thin film of Vaseline. Unable to transmit a tensile force through the joint, the time-piece would become detached from the main HPB once the magnitude of the reflected pulse (the original compressive wave reflected as a tensile wave off the free distal end of the time-piece) exceeded that of the incoming compressive wave, i.e. the net force at the joint transitioned to tension. From the momentum of the detached time-piece the mean pressure could be calculated.

Whilst this method is useful for measuring loads over extremely short durations, it cannot be used to provide any temporal characteristics of the applied pressure and only gives a time-averaged value. Multiple experiments could be performed with differing time-piece lengths to calculate the average pressure over different durations and hence determine an aggregate pressure-time history, but this requires great experimental effort. Davies (1948) was the first researcher to present dynamic axial and radial strain measurements using parallel plate and cylindrical condensers in conjunction with a double beam cathode-ray oscillograph. This allowed the pressure-time history to be inferred directly from the experimental data, albeit with some manipulation¹. In more recent HPB experiments, axial and/or radial strain in the bar is most frequently measured using electrical resistance or semi-conductor strain gauges mounted on the bar perimeter, e.g. Puckett & Peterson (2005a,b), Cloete & Nurick (2016), Rigby et al. (2015, 2016), Tyas & Ozdemir (2014), Tyas et al. (2016).

3.2 The Kolsky bar

A variation of the HPB, known as the split Hopkinson pressure bar (SHPB) or Kolsky bar after its creator (Kolsky 1949), was developed for the determination of the mechanical properties of different materials at high strain rates. In this arrangement, a thin specimen is located between two cylindrical HPBs (hence the term ‘split’) and a stress pulse is applied to the end of one of the bars termed the ‘incident’ or ‘input’ bar. As this stress pulse reaches the interface between the incident bar and the sample, it is partially transmitted through the sample into the second bar, termed the ‘transmitter’ or ‘output’ bar, and partially reflected back into the incident bar. With knowledge of the temporal variation of the original, transmitted and reflected stress waves, the stress-time and strain-time (and hence strain rate-time) response of the sample can be calculated, again using one-dimensional stress wave theory. From this, the material stress-strain behaviour at a known strain rate can be derived. These calculations are omitted from this article for brevity, however detailed derivation is available in Gray (2000).

The SHPB is a widely-used apparatus for high strain-rate material characterisation. A *Scopus* search for the terms ‘split Hopkinson pressure bar’ and ‘Kolsky bar’ reveals that 2,995 articles were published between 2011 and 2015 containing either term; a yearly average of almost 600 publications which use the SHPB apparatus. It is not the purpose of this article to review current research using the SHPB technique; it is instead focused on the HPB in its original form as a dynamic force transducer, and the applications and limitations of this technique from a civil engineering perspective. For a more detailed overview of recent SHPB work, the reader is directed to the review paper by Gama et al. (2004).

4 Three-dimensional elastic wave propagation

4.1 First mode propagation theory

Pochhammer (1876) and Chree (1889) independently formulated the equation of motion in cylindrical coordinates for the propagation of a sinusoidal wave of frequency f through an infinite-length, homogeneous, isotropic cylinder of uniform cross-section. A frequency equation was derived by applying traction-free boundary conditions on the surface of the bar and is presented in detail by Love (1927) and solved numerically by Bancroft (1941). The frequency equation, often termed the Pochhammer-Chree (PC) equation, takes the following form:

$$(x - 1)^2\Phi(ha) - (\beta x - 1)[x - \Phi(ka)] = 0 \quad (7)$$

where

$$\begin{aligned} x &= (C_p/C_0)^2(1 + \nu) \\ \beta &= (1 - 2\nu)(1 - \nu) \\ h &= \gamma\sqrt{(\beta x - 1)} \\ k &= \gamma\sqrt{(2x - 1)} \\ \Phi(y) &= yJ_0(y)/J_1(y) \end{aligned}$$

¹The experimental arrangement detailed in Davies (1948) measured longitudinal displacement at the end of the bar and radial displacement of the surface of the bar with time. Using one-dimensional stress wave theory, Davies was able to link the longitudinal particle velocity and radial displacement to the stress in the bar, i.e. the applied pressure

and a , C_0 , C_p , L and ν are bar radius, longitudinal wave velocity, phase velocity, wavelength, and Poisson's ratio as introduced previously, $J_n(y)$ is a Bessel function of the first kind, order n , and γ is the wave number, $\gamma = 2\pi/L$.

This equation can be solved either numerically by implementing a suitable root finding algorithm such as the bisection or Newton-Raphson method, or graphically following the method introduced by Honarvar et al. (2009). Figure 5 shows how the magnitude of the left hand side of equation 7 varies with normalised phase velocity, C_p/C_0 , for a constant ratio of bar radius to wavelength, $a/L = 0.1$, and constant Poisson's ratio, $\nu = 0.3$.

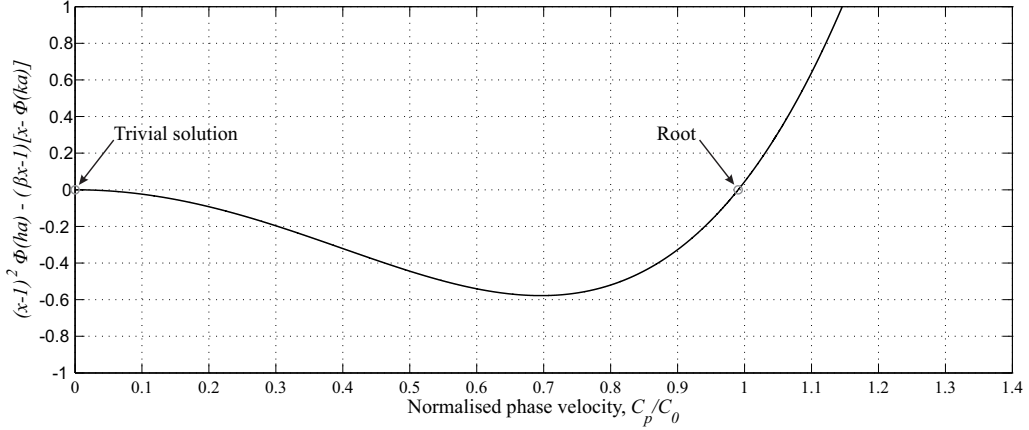


Figure 2: Roots of the Pochhammer-Chree frequency equation (7) for $a/L = 0.1$ and $\nu = 0.3$

Whilst the PC equation produces a trivial solution at $C_p/C_0 = 0$ for all values of a/L , it can be seen that for this value of a/L , the first non-trivial root of the PC equation lies at $C_p/C_0 = 0.9905$, i.e. an infinite sinusoid with wavelength $10a$ will propagate at a velocity very close to the bar velocity, C_0 .

Given a root of the PC equation for a particular value of a/L , the normalised group velocity, C_g/C_0 , can be determined using the following expression (Davies 1948)

$$\frac{C_g}{C_0} = \frac{C_p}{C_0} + \frac{a}{L} \frac{d(C_p/C_0)}{d(a/L)} \quad (8)$$

Here the phase velocity describes the velocity of transmission of surfaces of constant phase, and the group velocity describes the propagation velocity of a wave packet of constant (or near-constant) wavelength (Davies 1948). The group velocity is generally of higher importance when considering stress wave propagation as this is velocity at which energy propagates.

The frequency can be related to the wavelength through the following expression,

$$C_p = Lf \quad (9)$$

and hence the roots of the PC equation can be used to plot normalised group/phase velocity versus normalised frequency, fa/C_0 , as in Figure 3.

Any longitudinal stress pulse generated at the face of a HPB can be expressed as an infinite series of sinusoids of varying amplitude and frequency. It can be seen from Figure 3 that the solutions to the PC equation yield phase velocities that vary as a function of frequency, therefore whilst low-frequency components of a signal will propagate at approximately the bar velocity, higher frequency components of a signal will travel significantly slower. This means that a stress wave will *disperse* as it propagates along a cylindrical bar, particularly if the signal contains higher frequency components (short transients) as is often the case in the measurement of impact or blast pressures (Tyas & Watson 2001). Pochhammer-Chree dispersion was shown to occur in detailed experiments conducted by Davies (1948) and Zemanek Jr (1972), among others.

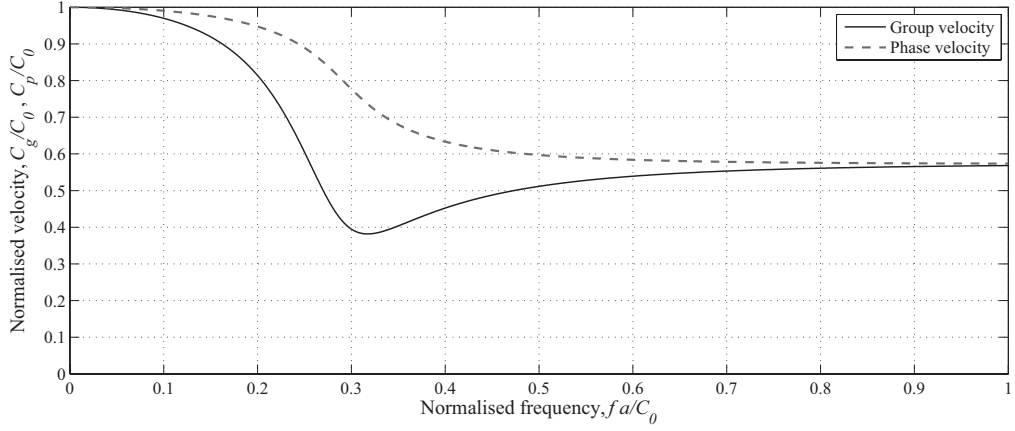


Figure 3: Normalised group and phase velocity versus normalised frequency (mode 1 only)

The effect of this dispersion is shown in Figure 4, which shows the stress distribution (black) along the length of stainless steel bar after a trapezoidal input pulse (grey) was propagated 2 m along the bar using the solutions of the PC equation (Barr 2016). In this example, the sharp leading and trailing edges of the signal initially contains high frequency components which subsequently lag behind the lower frequency components of the main body of the pulse as it propagates, and hence the signal becomes more rounded and high frequency oscillations are introduced immediately following the head and tail of the pulse.

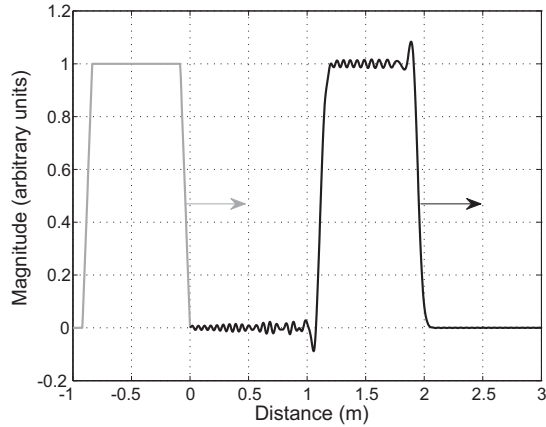


Figure 4: Dispersion of a trapezoidal wave after propagating 2 m along a cylindrical HPB (Barr 2016)

4.2 Multi-mode propagation theory

The PC equation is not defined by a single non-trivial solution; there are an infinite number of roots that satisfy the frequency equations. For lower frequencies there is a single real root which corresponds to the first mode of propagation, however with increasing frequency there exist multiple real roots of the PC equation. This means that higher frequency components of a signal will propagate in more than one mode, with each mode having a distinct phase velocity. Figure 5 shows the first three non-trivial roots of the PC equation for $a/L = 0.5$ and

$\nu = 0.3$. The values of these roots and their corresponding group velocities and normalised frequencies are given in Table 1.

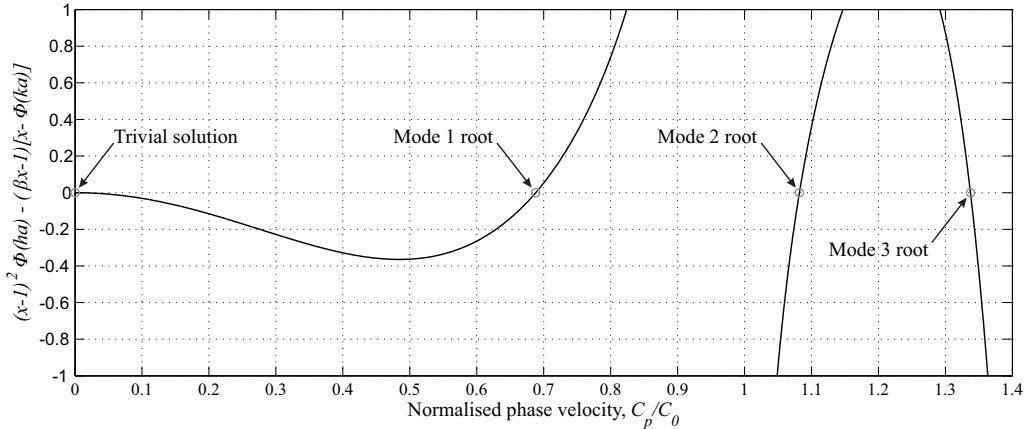


Figure 5: Roots of the Pochhammer-Chree frequency equation (7) for $a/L = 0.5$ and $\nu = 0.3$

	a/L	C_p/C_0	C_g/C_0	fa/C_0
Mode 1	0.5	0.68814	0.39782	0.34407
Mode 2	0.5	1.08195	0.79815	0.54098
Mode 3	0.5	1.33742	0.64956	0.66871

Table 1: Roots of the Pochhammer-Chree frequency equation (7) for $\nu = 0.3$ as in Figure 5, with corresponding values of normalised group velocity, C_g/C_0 , and normalised frequency, fa/C_0

The first ten roots of the PC equation are plotted as normalised phase and normalised group velocity curves in Figure 6 and 7 respectively. These are commonly referred to as the Pochhammer-Chree dispersion curves. Here, the PC equation was solved numerically following a procedure similar to that of Bancroft (1941). For each value of radius-to-wavelength, a/L , the lowest ten values of x which satisfy the PC equation were found for constant β and γ using the bisection method (as in Figures 2 and 5 albeit on an extended horizontal axis). Roots were determined for values of radius-to-wavelength in the range $0 \leq a/L \leq 4$ at intervals of $\Delta a/L = 0.0005$.

It can be seen in Figure 7 that for each mode other than mode 1, there exists a frequency below which the mode becomes non-propagating, i.e. the point at which wave number is equal to zero and thus the phase velocity is infinite. This is known as the ‘cut-off frequency’.

Curtis (1954) was the first to experimentally observe second-mode dispersion in a cylindrical bar. Here, a HPB was placed at the end of a shock tube and a step-like loading function was generated through reflection of a shock generated in the tube off the end of the HPB. Whilst the expected oscillations were seen to follow the head of the recorded stress pulse (recorded by a perimeter mounted strain gauge), a second set of high frequency oscillations were seen to ‘interrupt’ the first-mode oscillations. The velocities of each frequency packet were seen to agree reasonably well with the group velocities predicted by PC theory. Oliver (1957) provided further evidence of the second mode, and detected a phenomenon termed ‘edge resonance’. When a pulse is applied to the end of a HPB the majority of the energy propagates axially along the bar. A small fraction of the energy, however, remains at the loaded end of the bar in a very narrow frequency band. The energy of this resonant mode gradually leaks into the HPB as a normal propagating mode. Indeed, Kolsky (1954) observed this resonant mode and attributed it to axial propagation at the lowest of the mode 2 group velocities, i.e. those belonging to frequencies immediately greater than the cut-off frequency of the second mode. In later experiments, Curtis (1960) was able to observe the first six PC modes.

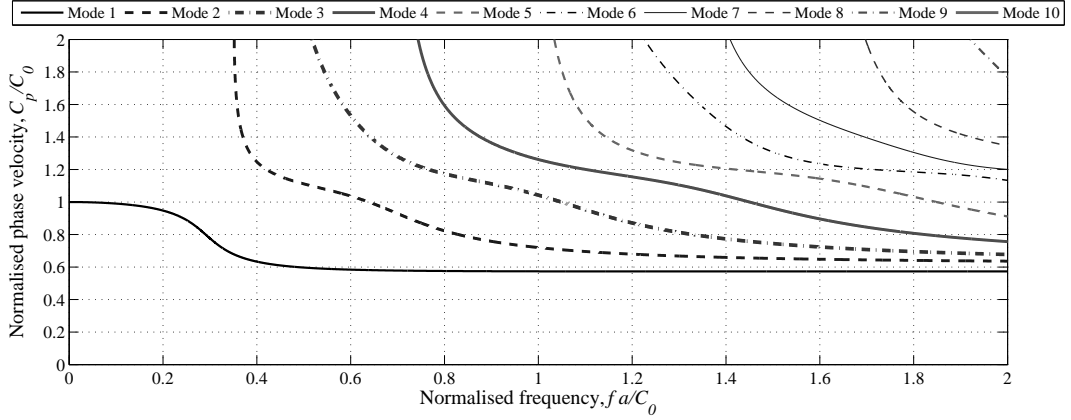


Figure 6: Normalised phase velocity versus normalised frequency for modes 1–10, $\nu = 0.30$ (phase velocity for mode 10 not visible on these axes)

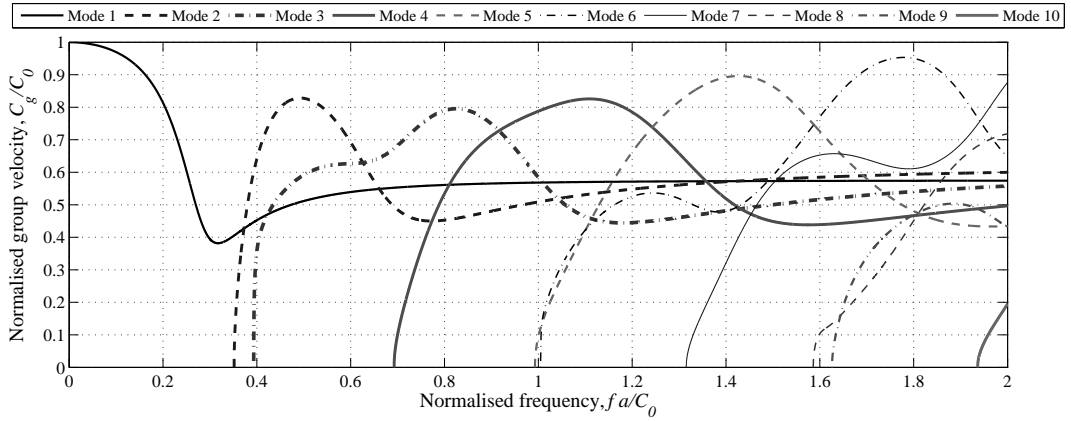


Figure 7: Normalised group velocity versus normalised frequency for modes 1–10, $\nu = 0.30$

4.3 Novel use of dispersion curves

Guided wave testing is a recent advancement in non-destructive assessment of materials and structures that draws heavily on the dispersion curves derived from PC theory. Given a bar (often termed a ‘waveguide’ as the stress waves propagate within the boundaries of the bar) of known material property and geometry, an acoustic or ultrasonic wave should disperse as it propagates axially through the bar in a manner predicted by the PC frequency equation. If the wave encounters either a change in cross-sectional area or local stiffness (e.g. it encounters an imperfection) then it will partially reflect back to the source of the wave. Given the arrival time of the reflection and knowledge of the wave velocity from solution of the PC equation, the location of the imperfection can be determined.

Several recent advancements have been made in the field of guided wave testing. As PC theory assumes the case of a bar situated in a vacuum the attenuation into the surrounding material is assumed to be zero. This approximation is valid for bars in air, however when the bar is surrounded by a dense fluid or a solid then leakage into the surrounding material becomes significant. Pavlakovic et al. (2001) studied the dispersion behaviour of steel bars embedded in grout in order to detect damage in steel tendons in post-tensioned concrete bridges. This also has applications for damage detection in buried pipelines (Leinov et al. 2016).

The three-dimensional PC theory described in Section 4.1 above assumes the situation of an elastic wave propagating through a cylindrical bar. Hayashi et al. (2003) demonstrated how wave dispersion behaviour can be predicted for bars of arbitrary cross-section, thus allowing for rapid non-destructive testing of large structures with complex cross-sections, such as railway tracks. Farhidzadeh & Salamone (2015) presented a method for estimating the loss of cross sectional area using PC dispersion curves in order to evaluate corrosion damage in steel strands in structures such as cable-stayed bridges, prestressed concrete structures, and re-centering systems. This work was developed by Treyssède (2016) to take into account the helical and multi-wire structure of strands.

Subhani et al. (2013) studied guided wave propagation through orthotropic media in cylindrical structures, e.g. timber poles. Updated dispersion curves are presented alongside traditional PC curves which assume propagation through isotropic media. The results are used to demonstrate the importance of consideration of fibre orientation in a timber pole when studying wave propagation.

5 Mode 1 dispersion correction

5.1 Frequency domain correction

In some applications, such as SHPB testing, it is possible to shape the loading pulse such that dispersion effects are minimised (Cloete et al. 2014). When the HPB is used as a dynamic force transducer, however, the exact form of the load applied to the HPB is unknown and there is the need, therefore, to be able to faithfully reconstruct an input loading pulse from the experimentally measured values.

Gorham (1983) and Follansbee & Frantz (1983) independently developed a frequency domain method for dispersion correction of pressure bar signals. This approach has since become widely accepted as the most accurate and valid first-mode dispersion correction and is detailed below:

- Convert a time-domain signal into the frequency domain using a fast Fourier transform (FFT) algorithm or similar
- Determine phase angle, ϕ , of each frequency component
- Calculate the phase velocity, C_p , of each frequency component
- For a signal that has propagated an axial distance of Δz , the phase shift, ϕ' , can be determined from the component frequency, f , and phase velocity:

$$\phi' = \left(\frac{C_0}{C_p} - 1 \right) \frac{2\pi f \Delta z}{C_0} \quad (10)$$

- Apply a phase angle correction to each frequency component

$$\phi_{corr} = \phi - \phi' \quad (11)$$

- Convert the corrected signal back into the time domain using an inverse FFT or similar

Gong et al. (1990), Lee & Crawford (1993), Lifshitz & Leber (1994), Zhao & Gary (1997), Marais et al. (2004) and Cloete & Nurick (2016), among others, have used this method to adequately correct for dispersion effects in HPB and SHPB signals.

5.2 Variation along a radial ordinate

As well as the frequency dependent dispersion predicted by the PC analysis, the work of Davies (1948) showed that a propagating signal will be affected in at least two additional ways. Firstly, lateral inertia will cause the magnitude of the stress to vary across the radial ordinate of the bar. Secondly, the ratio of axial stress to axial strain (i.e. the Young's modulus of elasticity of the HPB) will not be constant across the bar cross-section and

varies with both frequency and radial ordinate. Thus experimental signals recorded on the perimeter of a HPB will not be representative of the axial stress propagating through the bar and, in addition to PC dispersion correction, must also be corrected to account for these additional errors.

The importance of the frequency dependence of the amplitude of a propagating signal was discussed by Safford (1992). Tyas & Watson (2000) experimentally demonstrated this variation by comparing the magnitude of measured axial and radial strain. The results were found to demonstrate excellent agreement with PC theory at low frequencies, however the agreement was seen to become less clear with the introduction of higher modes of propagation.

Through manipulation of Davies' equations, Tyas & Watson (2001) were able to derive two correction factors, termed M_1 and M_2 , which can be used to convert the surface strain to average axial strain, and average axial strain to average axial stress respectively. The two correction factors, using the same notation as equation 7, are given as follows:

$$M_1 = \frac{2 \left(1 + \frac{1 - \beta x}{x - 1} \right)}{\Phi(ha) + \Phi(ka) \frac{1 - \beta x}{x - 1}} \quad (12)$$

and

$$M_2 = E \left(\frac{C_p}{C_0} \right)^2 \quad (13)$$

These correction factors are presented graphically for mode 1 propagation and $\nu = 0.29$ in Figure 8. Tyas & Watson (2001) go on to state that the values of M_1 and M_2 are relatively insensitive to changing Poisson's ratio for values of radius:wavelength less than 0.3, and that correction factors for higher mode propagation can also be calculated by substituting the relative phase velocity data.

The strength of this method is that it is compatible with the Gorham (1983)/Follansbee & Frantz (1983) frequency domain correction method. In addition to the traditional phase shift correction, the magnitude of each frequency component need only be multiplied by the corresponding values of M_1 and M_2 to achieve full amplitude and phase correction. The method was verified numerically in the original paper, and later experimentally validated (Tyas & Pope 2005).

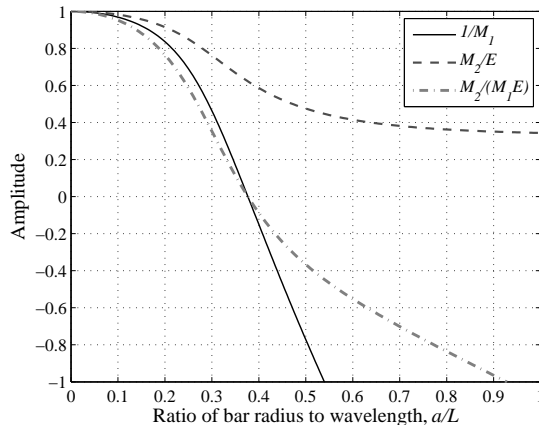


Figure 8: M_1 and M_2 correction factors for mode 1 propagation, $\nu = 0.29$ (Tyas & Watson 2001)

6 Higher mode dispersion correction

Using an FFT to express an input function as a series of sine waves gives information only of the amplitude and phase shift of *each Fourier component*. At normalised frequencies greater than the mode 2 cut-off frequency, a single Fourier component will represent a combination of *at least two* separate sinusoids with the same carrier frequency, but with different amplitudes, travelling at different velocities as predicted by PC theory. Because of this, the phase shift/amplitude correction methods introduced previously only work for the first mode. With higher modes of propagation, it is currently not known exactly how much energy propagates in each mode at a particular frequency, and it is therefore not possible to accurately correct for dispersion beyond the cut-off frequency of mode 2.

Several authors have studied the higher mode features of PC theory. Lee & Crawford (1993) developed a new method for analysing data recorded from HPB experiments, termed a Gaussian-windowed Fourier transform (GWFT), to calculate the arrival time of each Fourier component and hence determine group velocity. Following on from this, Lee et al. (1995) used a series of different GWFTs, each with a different time interval, to develop Fourier coefficients, i.e. the ‘strength’ of a particular frequency within that time interval. When plotted against normalised frequency, the Fourier coefficients were seen to form ‘power bands’. These power bands followed the contours of the theoretical PC modes, and each mode was dominant (more powerful) when its group velocity exceeded the velocities of all other modes, which can be seen in Figure 4 in Lee et al. (1995).

Using this information, Puckett (2004) and Husemeyer (2011) formulated higher mode dispersion correction algorithms. The former using a series of transfer functions to model the relative amplitude of each mode at higher frequencies, with each mode being dominant over a small frequency range, while the latter assumed that each mode contributes fully when its group velocity is greater than that of all other modes, and does not contribute at any other frequency.

Whilst these studies offer valuable insights into the behaviour of PC dispersion at higher modes, it is generally accepted that an exact higher mode dispersion correction methodology has not yet been formulated. In order for engineers to be able to capture transients in the order of micro- to milliseconds typically associated with the leading edge of a shock front, higher PC modes are becoming an increasingly important consideration.

7 Summary and conclusions

The Hopkinson pressure bar, named after its creator Bertram Hopkinson (1914), was devised as a method for measuring high-energy, transient loads. After application of a dynamic load on the end of a HPB, an elastic stress pulse propagates along its length. Fixing a semi-conductor strain gauge, as an example, at some distance from the face of the HPB enables the experimentalist to both record the loading event and also protect sensitive equipment. The HPB is therefore a valuable tool for measuring extreme loading events relevant to civil and structural engineering applications, such as the detonation of an explosive located close to a structural column.

This paper reviews the applications and limitations of the HPB. The longitudinal wave velocity is derived for the case of one-dimensional elastic waves propagating along an infinite length bar. The analysis of Pochhammer (1876) and Chree (1889) is introduced, which considers the propagation of sinusoidal wavetrains through a cylinder. The PC analysis, as it is referred to in this paper, demonstrates that the phase velocity of a harmonic wave is a function of its wavelength, and therefore any signal will disperse as it propagates along a HPB as its frequency components move out of phase.

The well-known frequency domain dispersion correction method of Follansbee & Frantz (1983) is presented, as well as additional corrections based on the distribution of axial strain across the bar radius, and the changing (dynamic) Poisson’s ratio across the bar radius, after Tyas & Watson (2001).

At lower frequencies, each sinusoid will travel at a single velocity as predicted by PC theory. Any frequencies above a certain value, known as the mode 2 cut-off frequency, will propagate at more than one velocity. The apportioning of energy in multiple-mode propagation is currently unknown, and dispersion correction algorithms are presently only accurate below the mode 2 cut-off. Research into this area is ongoing at the University of Sheffield. Higher mode dispersion correction is a necessary requirement to allow sub-microsecond features of high explosive blast loading to be resolved. Once this is available, it will improve our understanding of the

fundamental mechanisms of blast loading and allow civil and structural engineers to more safely and efficiently design blast resilient infrastructure.

Acknowledgements

This work forms part of a project that was joint-funded by The Defence Science and Technology Laboratory and the Institution of Civil Engineers Research and Development Enabling Fund.

References

- Bancroft, D. (1941), ‘The velocity of longitudinal waves in cylindrical bars’, *Physical Review* **59**, 588–593.
- Barr, A. (2016), Strain-rate effects in quartz sand, PhD thesis, Department of Civil & Structural Engineering, University of Sheffield, UK.
- Chree, C. (1889), ‘The equations of an isotropic elastic solid in polar and cylindrical co-ordinates’, *Transactions of the Cambridge Philosophical Society* **14**, 250–369.
- Clarke, S., Fay, S., Warren, J., Tyas, A., Rigby, S. & Elgy, I. (2015), ‘A large scale experimental approach to the measurement of spatially and temporally localised loading from the detonation of shallow-buried explosives’, *Measurement Science and Technology* **26**, 015001.
- Cloete, T. J., Paul, G. & Ismail, E. B. (2014), ‘Hopkinson bar techniques for the intermediate strain rate testing of bovine cortical bone’, *Philosophical Transactions of the Royal Society of London A: Mathematical, Physical and Engineering Sciences* **372**(2015), 20130291.
- Cloete, T. & Nurick, G. (2016), ‘Blast characterization using a ballistic pendulum with a centrally mounted Hopkinson bar’, *International Journal of Protective Structures* **7**(3), 367–388.
- Cormie, D., Mays, G. & Smith, P. (2009), *Blast effects on buildings, 2nd ed.*, Thomas Telford, London, UK.
- Curtis, C. (1954), ‘Second Mode Vibrations of the Pochhammer-Chree Frequency Equation’, *Journal of Applied Physics* **25**(7), 928.
- Curtis, C. (1960), Propagation of an elastic pulse in a semi-infinite bar, in ‘Proceedings of the International Symposium on Stress Wave Propagation in Materials’, Pennsylvania State University, USA.
- Davies, R. (1948), ‘A critical study of the Hopkinson Pressure Bar’, *Philosophical Transactions of the Royal Society of London. Series A, Mathematical and Physical Sciences* **240**(821), 375–457.
- Farhidzadeh, A. & Salamone, S. (2015), ‘Reference-free corrosion damage diagnosis in steel strands using guided ultrasonic waves’, *Ultrasonics* **57**(2015), 198–208.
- Fay, S., Rigby, S., Tyas, A., Clarke, S., Reay, J., Warren, J. & Brown, R. (2015), ‘Displacement timer pins: An experimental method for measuring the dynamic deformation of explosively loaded plates’, *International Journal of Impact Engineering* **86**, 124–130.
- Follansbee, P. & Frantz, C. (1983), ‘Wave propagation in the Split Hopkinson Pressure Bar’, *Journal of Engineering Materials and Technology* **105**, 61–66.
- Gama, B., Lopatnikov, S. & Gillespie, J. (2004), ‘Hopkinson Bar experimental technique: A critical review’, *Applied Mechanics Reviews* **57**(4), 223–249.
- Gong, J., Malvern, L. & Jenkins, D. (1990), ‘Dispersion investigation in the Split Hopkinson Pressure Bar’, *Journal of Engineering Materials and Technology* **112**, 309–314.

- Gorham, D. (1983), ‘A numerical method for the correction of dispersion in pressure bar signals’, *Journal of Physics E: Scientific Instruments* **16**, 477–479.
- Gray, G. (2000), *Classic Split-Hopkinson Pressure Bar testing. ASM Handbook Volume 8, Mechanical Testing and Evaluation*, ASM International, Ohio, USA.
- Hayashi, T., Song, W.-J. & Rose, J. (2003), ‘Guided wave dispersion curves for a bar with an arbitrary cross-section, a rod and rail example’, *Ultrasonics* **41**(3), 175–183.
- Honarvar, F., Enjilela, E. & Sinclair, A. (2009), ‘An alternative method for plotting dispersion curves’, *Ultrasonics* **49**(1), 15–18.
- Hopkinson, B. (1914), ‘A method of measuring the pressure produced in the detonation of high explosives or by the impact of bullets’, *Philosophical Transactions of the Royal Society of London. Series A, Containing Papers of a Mathematical or Physical Character* **213**(1914), 437–456.
- Husemeyer, P. (2011), Theoretical and numerical investigation of multiple-mode dispersion in Hopkinson bars, PhD thesis, Blast Impact and Survivability Research Unit, Department of Mechanical Engineering, University of Cape Town, South Africa.
- Hyde, D. W. (1991), *Conventional Weapons Program (ConWep)*, U.S Army Waterways Experimental Station, Vicksburg, MS, USA.
- Kolsky, H. (1949), ‘An investigation of the mechanical properties of materials at very high rates of loading’, *Proceedings of the Physical Society. Section B* **62**(11), 676.
- Kolsky, H. (1954), ‘The propagation of longitudinal elastic waves along cylindrical bars’, *The London, Edinburgh, and Dublin Philosophical Magazine and Journal of Science* **45**(366), 712–726.
- Kolsky, H. (1963), *Stress waves in solids, 1963 ed.*, Dover Publications, New York, USA.
- Landon, J. & Quinney, H. (1923), ‘Experiments with the Hopkinson Pressure Bar’, *Proceedings of the Royal Society of London A: Mathematical, Physical and Engineering Sciences* **103**(723), 622–643.
- Lee, C. & Crawford, R. (1993), ‘A new method for analysing dispersed bar gauge data’, *Measurement Science and Technology* **4**, 931–937.
- Lee, C., Crawford, R., Mann, K., Coleman, P. & Petersen, C. (1995), ‘Evidence of higher Pochhammer-Chree modes in an unsplit Hopkinson Bar’, *Measurement Science and Technology* **6**, 853–859.
- Leinov, E., Lowe, M. J. & Cawley, P. (2016), ‘Ultrasonic isolation of buried pipes’, *Journal of Sound and Vibration* **363**, 225 – 239.
- Lifshitz, J. & Leber, H. (1994), ‘Data processing in the split Hopkinson pressure bar tests’, *International Journal of Impact Engineering* **15**(6), 723 – 733.
- Love, A. (1927), *A treatise on the mathematical theory of elasticity, 4th edn.*, Cambridge University Press, UK.
- Marais, S., Tait, R., Cloete, T. & Nurick, G. (2004), ‘Material testing at high strain rate using the split Hopkinson pressure bar’, *Journal of Applied Mechanics* **1**(3), 319–339.
- Oliver, J. (1957), ‘Elastic Wave Dispersion in a Cylindrical Rod by a Wide-Band Short-Duration Pulse Technique’, *The Journal of the Acoustical Society of America* **29**(2), 189–194.
- Pavlakovic, B., Lowe, M. & Cawley, P. (2001), ‘High-frequency low-loss ultrasonic modes in imbedded bars’, *Journal of Applied Mechanics* **68**(1), 67–75.
- Pochhammer, L. (1876), ‘Über die fortpflanzungsgeschwindigkeiten kleiner schwingungen in einem unbegrenzten isotropen kreiszylinder’, *Journal für die reine und angewandte Mathematik* **81**, 324–336.

- Puckett, A. (2004), An experimental and theoretical investigation of axially symmetric wave propagation in thick cylindrical waveguides, PhD thesis, The Graduate School, The University of Maine, USA.
- Puckett, A. & Peterson, M. (2005a), ‘Individual longitudinal Pochhammer-Chree modes in observed experimental signals’, *Acoustics Research Letters Online* **6**(4), 268–273.
- Puckett, A. & Peterson, M. (2005b), ‘A semi-analytical model for predicting multiple propagating axially symmetric modes in cylindrical waveguides’, *Ultrasonics* **43**(3), 197–207.
- Rigby, S., Fay, S., Clarke, S., Tyas, A., Reay, J., Warren, J., Gant, M. & Elgy, I. (2016), ‘Measuring spatial pressure distribution from explosives buried in dry Leighton Buzzard sand’, *International Journal of Impact Engineering* **96**(2016), 89–104.
- Rigby, S., Tyas, A., Clarke, S., Fay, S., Reay, J., Warren, J., Gant, M. & Elgy, I. (2015), ‘Observations from Preliminary Experiments on Spatial and Temporal Pressure Measurements from Near-Field Free Air Explosions’, *International Journal of Protective Structures* **6**(2), 175–190.
- Robertson, R. (1921), ‘Some properties of explosives’, *Journal of the Chemical Society, Transactions* **119**, 1–29.
- Safford, N. (1992), Materials testing up to 10^5 s^{-1} using a minaturised Hopkinson Bar with dispersion corrections, in ‘Proceedings of the International Symposium on Intense Dynamic Loading and its Effects’, Chengdu, China.
- Shin, J., Whittaker, A. S. & Cormie, D. (2015), ‘Incident and normally reflected overpressure and impulse for detonations of spherical high explosives in free air’, *Journal of Structural Engineering* **04015057**(13), 1–13.
- Shin, J., Whittaker, A. S., Cormie, D. & Wilkinson, W. (2014), ‘Numerical modeling of close-in detonations of high explosives’, *Engineering Structures* **81**, 88–97.
- Subhani, M., Li, J. & Samali, B. (2013), ‘A comparative study of guided wave propagation in timber poles with isotropic and transversely isotropic material models’, *Journal of Civil Structural Health Monitoring* **3**(2), 65–79.
- Treysède, F. (2016), ‘Dispersion curve veering of longitudinal guided waves propagating inside prestressed seven-wire strands’, *Journal of Sound and Vibration* **367**, 56–68.
- Tyas, A. & Ozdemir, Z. (2014), ‘On backward dispersion correction of Hopkinson Pressure Bar signals’, *Philosophical Transactions of the Royal Society of London. Series A, Mathematical, Physical and Engineering Sciences* **372**, 20130291.
- Tyas, A. & Pope, D. (2005), ‘Full correction of first-mode Pochhammer-Chree dispersion effects in experimental pressure bar signals’, *Measurement Science and Technology* **16**(3), 642–652.
- Tyas, A. & Watson, A. (2000), ‘Experimental evidence of Pochhammer-Chree strain variations in elastic cylinders’, *Experimental Mechanics* **40**(3), 331–337.
- Tyas, A. & Watson, A. (2001), ‘An investigation of frequency domain dispersion correction of pressure bar signals’, *International Journal of Impact Engineering* **25**(1), 87–101.
- Tyas et al. (2016), ‘Experimental studies of the effect of rapid afterburn on shock development of near-field explosions’, *International Journal of Protective Structures* **7**(3), 456–465.
- US Department of Defence (2008), *Structures to resist the effects of accidental explosions*, US DoD, Washington DC, USA, UFC-3-340-02.
- Zemanek Jr, J. (1972), ‘An experimental and theoretical investigation of elastic wave propagation in a cylinder’, *The Journal of the Acoustical Society of America* **51**, 265–283.
- Zhao, H. & Gary, G. (1997), ‘A new method for the separation of waves. Application to the SHPB technique for an unlimited duration of measurement’, *Journal of the Mechanics and Physics of Solids* **45**(7), 1185 – 1202.